An Extended Harmonic Balance Method based on Incremental Nonlinear Control Parameters

Hamed Haddad Khodaparast[1], Hadi Madinei[1], Michael I. Friswell[1], Sondipon Adhikari[1], Simon Coggon[2], Jonathan E. Cooper[3]

Abstract

A new formulation for calculating the steady-state responses of multiple-degree-of-freedom (MDOF) non-linear dynamic systems due to harmonic excitation is developed. This is aimed at solving multi-dimensional nonlinear systems using linear equations. Nonlinearity is parameterised by a set of 'non-linear control parameters' such that the dynamic system is effectively linear for zero values of these parameters and nonlinearity increases with increasing values of these parameters. Two sets of linear equations which are formed from a first-order truncated Taylor series expansion are developed. The first set of linear equations provides the summation of sensitivities of linear system responses with respect to non-linear control parameters and the second set are recursive equations that use the previous responses to update the sensitivities. The obtained sensitivities of steady-state responses are then used to calculate the steady state responses of non-linear dynamic systems in an iterative process. The application and verification of the method are illustrated using a non-linear Micro-Electro-Mechanical System (MEMS) subject to a base harmonic excitation. The non-linear control parameters in these examples are the DC voltages that are applied to the electrodes of the MEMS devices.

Keywords: MDOF Non-linear dynamics, sensitivity,

[1]College of Engineering, Swansea University, Bay Campus, Fabian Way, Swansea SA1 8EN, United Kingdom
[2]Airbus Operations Ltd., New Filton House, Bristol BS99 7AR, United Kingdom
[3]Department of Aerospace Engineering, University of Bristol, Bristol BS8 1TR, United Kingdom

1. Introduction

Vibration analysis of structures containing nonlinearities is one of the important topics in structural engineering problems. There are many practical engineering components that are modeled as nonlinear oscillatory systems. In most cases, the nonlinear dynamics of these systems have been investigated through numerical methods such as the Newmark method, the shooting method, the differential quadrature method and the Adomian decomposition method [1, 2, 3, 4]. Using these simulations to study the effect of different parameters on the dynamics of the system is always time consuming, particularly for multi-dimensional non-linear systems and the cases where the sensitivities of responses are required. Therefore obtaining the steady state solution of multiple-degree-of-freedom non-linear dynamic systems is of great importance in this field. A comprehensive account of nonlinear structural dynamics and control is given by Wagg and Neild [5].

In order to investigate the analytical solution of nonlinear structures, different techniques have been applied in the literature. The Max-min [6], the parameter-expanding approach[7], frequency-amplitude formulation [8], the Variational Iteration [9], perturbation techniques [10, 11, 12], the iteration perturbation [13], the Homotopy Analysis [14, 15], the Energy Balance analysis [16], the harmonic balance [17], the equivalent linearization method (ELM) [18, 19] and the Extended Lindstedt-Poincare approach [20] are some examples of these techniques. Each of these methods has some strong points and some weakness. The perturbation methods have been used for both weakly and strongly nonlinear problems (e.g. [21, 22]) and they are expressed by a series of perturbation quantities. Based on these quantities, the original nonlinear equations are replaced by linear equations (sometimes even nonlinear), which are specified by the original equation and also by the place where the perturbation quantities appear. Methods such as Homotopy Analysis, Variational Iteration, Energy Balance and

harmonic balance are also suitable for dealing with strong nonlinear problems. Qian et al. [14] studied the oscillation of a MEMS microbeam with strong nonlinearity by means of the Homotopy Analysis Method. They demonstrated that the method has good performance in investigating the nonlinear equation of the model studied in the paper. Fesanghary et al. [23] utlised a variational iterative method and proposed a new analytical approximation for the Duffing-harmonic oscillator. Their solution was valid in the whole range of oscillation amplitude variations; but it contained many harmonic terms. Younesian et al. [8] investigated the generalized Duffing equation using a frequency-amplitude formulation and energy balance method. They obtained the general solution for any arbitrary type of nonlinearity and showed that these two techniques are quite reliable even in strongly nonlinear systems. Peng et al. [24] applied the harmonic balance method to study the effects of cubic nonlinear damping on the performance of passive vibration isolators. Harmonic balance has been used to predict the steady-state solution of structures with different types of nonlinearity and also can be used for identification and health monitoring of nonlinear systems. There are several developments of the harmonic balance method such as incremental harmonic balance [25, 26], Newton harmonic balance [27], adaptive harmonic balance [28], residue harmonic balance [29], and Global residue harmonic balance [30]. Although these methods have been successfully used to obtain analytical solutions of different non-linear problems, there are few applications to multi-degree of freedom non-linear dynamic problems. In these problems, applying the aforementioned methods requires the solution of complicated non-linear algebraic equations which is really time consuming. Furthermore, in order to find the sensitivity of responses to non-linear parameters, additional computations are required.

This paper proposes an extended harmonic balance method for the steady-state solution of non-linear multiple-degree-of-freedom dynamic problems based on incremental nonlinear control parameters. The method only requires the solution of linear equations for the nonlinear problem. It also provides the sensitivities of the solution with respect to the nonlinear control parameters.

The nonlinear control parameters are those with which the non-linearity in the model is triggered. This property of nonlinear control parameters can be implemented in the solution of a nonlinear problem. They are incremented from zero to one (note that the parameters are normalised so that the maximum values are unity) and a linear equation giving the sensitivities of the responses with respect to the parameters is obtained at each increment. Using these sensitivities, the solution at each step can be calculated through the solution at the previous increment. The method starts from the linear system and continues until all nonlinear control parameters reach unity. The major advantages of the proposed method include the capability of solving smooth multi-dimensional nonlinear dynamic systems using linear equation solvers and the ability to obtain sensitivities that are useful in inverse problems such as vibration control and robust design. The application and verification of the method is demonstrated in a non-linear Micro-Electro-Mechanical System (MEMS) subject to a base harmonic excitation. The non-linearity is due to the electrostatic forces and the nonlinear control parameters are the DC voltages. The method is verified using numerical integration and some interesting results from the frequency responses of sensitivities are demonstrated and discussed.

2. Theory

Consider a damped structural dynamic system, defined on the domain $\mathcal{D} \in \mathbb{R}^d$ $(d \leq 3)$ with piecewise Lipschitz boundary $\partial\mathcal{D}$, subject to an externally applied harmonic excitation with the distributed forcing function $f(\mathbf{r})$. The governing equation may be cast in the form of the following general partial differential equation

$$\rho(\mathbf{r}) \frac{\partial^2 w(\mathbf{r},t)}{\partial t^2} + c(\mathbf{r}) \frac{\partial w(\mathbf{r},t)}{\partial t} + k(\mathbf{r}) \Gamma(w(\mathbf{r},t)) + f_{NL}\left(w(\mathbf{r},t), \bar{\boldsymbol{\theta}}\right) = \frac{f(\mathbf{r})}{2} \exp(i\Omega t) + cc. \tag{1}$$

with the usual mixture of Cauchy and Neumann boundary conditions on $\partial\mathcal{D}$. In the above equation (Eq.(1)), $w(\mathbf{r},t)$ is the displacement variable, where $\mathbf{r} \in \mathcal{D}$

is the spatial position vector and $t \in [0, T]$ is time, $\rho(\mathbf{r})$ is the distributed mass density, $c(\mathbf{r})$ is the distributed damping coefficient, $k(\mathbf{r})$ is the distributed stiffness parameter, Γ is a general differential operator, $f_{NL}\left(w(\mathbf{r},t), \bar{\boldsymbol{\theta}}\right)$ is the non-linear restoring force function with $\bar{\boldsymbol{\theta}} \in \mathbb{R}^m$ ($\bar{\boldsymbol{\theta}}$ includes the normalised non-linear control parameters $\mathbf{0} \leq \bar{\boldsymbol{\theta}} \leq \mathbf{1}$ and $f_{NL}(w, \mathbf{0}) = 0$), $i = \sqrt{-1}$, Ω is the excitation frequency and *cc.* denotes complex conjugate. Hereafter $w(\mathbf{r}, t)$, $f(\mathbf{r})$, $\rho(\mathbf{r})$, $c(\mathbf{r})$ and $k(\mathbf{r})$ are replaced by w, f, ρ, c and k for reasons of simplicity.

In this paper, it is assumed that the vector of nonlinear restoring force can be reasonably approximated by a limited number of terms of its Taylor series, i.e. H terms,

$$f_{NL}\left(w, \bar{\boldsymbol{\theta}}\right) \approx \sum_{h=0}^{H} \alpha_h\left(\bar{\boldsymbol{\theta}}\right) w^h \tag{2}$$

where $\alpha_h\left(\bar{\boldsymbol{\theta}}\right) = \frac{f_{NL}^{(h)}\left(0, \bar{\boldsymbol{\theta}}\right)}{h!}$, $f_{NL}^{(h)}$ denotes the hth derivative of f_{NL} evaluated at the point $w = 0$ and $\bar{\boldsymbol{\theta}}$, and $h!$ denotes the factorial of h.

The solution starts with the linear system when $f_{NL}\left(w, \bar{\boldsymbol{\theta}}\right) = 0$ in Eq.(1). In this case, the steady-state solution of the underlying dynamical system has the form

$$w_0 = \sum_{n=1}^{N} \varphi_n q_{n0} \exp(i\Omega t) + cc. \tag{3}$$

where $\varphi_n(\mathbf{r})\,(n = 1..N)$ (replaced by φ_n for simplicity) are linear normal mode shape functions that describe the spatial displacements and satisfy the boundary conditions, N is the number of shape functions that provide a good basis for prediction of the dynamic behaviour within the range of excitation frequency and q_{n0} are the amplitudes of steady-state responses. Substituting Eq.(3) into Eq.(1) (note that $f_{NL}\left(w, \bar{\boldsymbol{\theta}}\right) = 0$), applying the standard Galerkin approach and solving for $\mathbf{q}_0 = \{q_{n0}\} \in \mathbb{R}^N$ (note that $\exp(i\Omega t)$ is cancelled out from both sides) yields

$$\mathbf{q}_0 = \left[-\Omega^2 \mathbf{M} + i\Omega \mathbf{C} + \mathbf{K}\right]^{-1} \mathbf{F} \tag{4}$$

where $\mathbf{M} = [M_{ij}] \in \mathbb{R}^{N\times N}$, $\mathbf{C} = [C_{ij}] \in \mathbb{R}^{N\times N}$, $\mathbf{K} = [K_{ij}] \in \mathbb{R}^{N\times N}$ are the mass, damping and structural stiffness matrices of underlying linear system and $\mathbf{F} = \{F_j\} \in \mathbb{R}^N$ is the vector of force amplitudes and,

$$M_{ij} = \begin{cases} \int_{\mathcal{D}} \rho\varphi_i^2 d\mathbf{r} & \text{if} \quad i = j \\ 0 & \text{if} \quad i \neq j \end{cases} \tag{5}$$

$$C_{ij} = \begin{cases} \int_{\mathcal{D}} c\varphi_i^2 d\mathbf{r} & \text{if} \quad i = j \\ 0 & \text{if} \quad i \neq j \end{cases} \tag{6}$$

$$K_{ij} = \int_{\mathcal{D}} k\varphi_i \Gamma(\varphi_j) d\mathbf{r} \tag{7}$$

$$F_j = \int_{\mathcal{D}} \frac{f}{2}\varphi_j d\mathbf{r} \tag{8}$$

In this paper, space discretization is done by projecting the partial differential equation to the mode shapes of the underlying linear systems. This is not the only method for discretization and other methods such as finite element analysis can be also used. Now all of the normalised non-linear control parameters are equally perturbed by $\delta\bar{\theta}$ and therefore the steady state solution of Eq.(1) may be expressed as

$$w_1 = w_0 + \left(\sum_{j=1}^{m} \frac{\partial w_0}{\partial \bar{\theta}_j} \right) \delta\bar{\theta} + \mathcal{O}\left(\delta\bar{\theta}^2\right) \tag{9}$$

If $\delta\bar{\theta}$ is small enough, the higher order terms, $\mathcal{O}\left(\delta\bar{\theta}^2\right)$, can be ignored in Eq.(9). Assuming $\acute{w_1} = \sum_{j=1}^{m} \frac{\partial w_0}{\partial \bar{\theta}_j}$ and substituting Eq.(9) and Eq.(2) into Eq.(1), ignoring the higher orders of $\delta\bar{\theta}$ and cancelling out the linear equation from both sides gives:

$$\left(\rho \frac{\partial^2 \acute{w_1}}{\partial t^2} + c \frac{\partial \acute{w_1}}{\partial t} + k\Gamma\left(\acute{w_1}\right) \right) \delta\bar{\theta} + \sum_{h=0}^{H} \alpha_{1h} \left(w_0^h + h w_0^{h-1} \acute{w_1} \delta\bar{\theta} \right) = 0. \tag{10}$$

The choice of increments, i.e. equal increments, can be changed as there are many choices of paths through parameter space and this will be useful if

the sensitivities of the responses in different paths are sought. In the following equations $\alpha_{1h}\left(\bar{\boldsymbol{\theta}}\right)$ is replaced by α_{1h} for reasons of simplicity. The addition of the subscript 1 to α_h indicates its value at the first iteration. According to Eq.(10), the solution for $\acute{w_1}$ includes primary and higher harmonics of the excitation frequency. Therefore one may assume

$$\acute{w_1} = \sum_{l=1}^{L}\sum_{n=1}^{N} \varphi_n \acute{q}_{nl1} \exp\left(il\Omega t\right) + cc. \tag{11}$$

Substituting Eqs.(11) and (3) into Eq.(10), expanding all of the terms in Taylor series, balancing the harmonics of interest and applying the standard Galerkin technique, results in a set of linear equations of the form

$$\mathbf{A}_1 \acute{\mathbf{q}}_1 = \mathbf{b}_1 \tag{12}$$

in which the vector of unknowns $\acute{\mathbf{q}}_1 \in \mathbb{R}^{NL}$ includes the terms $\acute{q}_{nl1}$ where $n = 1, .., N$ and $l = 1, .., L$, the matrix $\mathbf{A}_1 \in \mathbb{R}^{NL\times NL}$ and the vector $\mathbf{b}_1 \in \mathbb{R}^{NL}$ consist of terms that are functions of the amplitudes of the steady-state responses of the linear system q_{n0}, systems parameters (ρ, c, k, $\boldsymbol{\theta}$), mode shapes (φ_n), the coefficients of the Taylor series in Eq.(2) α_{1h}, the perturbed non-linear control parameter $\delta\bar{\theta}$ and the excitation frequency Ω.

In the following, matrix $\mathbf{A}_1$ and vector $\mathbf{b}_1$ are obtained for the case when only the 'primary harmonics' of $\acute{w_1}$ are considered ($L = 1$) and the system contains an odd non-linearity ($h = 2k-1, k = 1, 2, ..., p$). This is the case in the numerical example that is used to illustrate the method. In this case,

$$\mathbf{A}_1 = \left[-\Omega^2\mathbf{M} + i\Omega\mathbf{C} + \mathbf{K} + \mathbf{E}^{(1)}\right]\delta\bar{\theta} \tag{13}$$

where $\mathbf{E}^{(1)} = [E_{ij}^{(1)}] \in \mathbb{R}^{N\times N}$,

$$E_{ij}^{(1)} = \int_{\mathcal{D}} \sum_{h=1}^{H} \left(h\alpha_{1h} \binom{h-1}{\frac{h-1}{2}} \left(\sum_{n=1}^{N} \varphi_n q_{n0}\right)^{\frac{h-1}{2}} \left(\sum_{n=1}^{N} \varphi_n q_{n0}^{*}\right)^{\frac{h-1}{2}} \right) \varphi_i\varphi_j d\mathbf{r} \tag{14}$$

where $\binom{\bullet}{\circ}$ is the binomial coefficient, and $\bullet^*$ indicates the complex conjugate of $\bullet$. The components of vector $\mathbf{b} = [b_i] \in \mathbb{R}^N$ are

$$b_{1i} = -\int_{\mathcal{D}} \sum_{h=1}^{H} \left(\alpha_{1h} \binom{h}{\frac{h-1}{2}} \left(\sum_{n=1}^{N} \varphi_n q_{n0} \right)^{\frac{h+1}{2}} \left(\sum_{n=1}^{N} \varphi_n q_{n0}^* \right)^{\frac{h-1}{2}} \right) \varphi_i d\mathbf{r} \quad (15)$$

Once the amplitudes of the sensitivities $\acute{\mathbf{q}}_1$ are obtained, the term $\acute{w}_1$ in Eq.(9) can be determined from Eq.(11) and consequently the steady state solution of weakly non-linear system w_1 is achieved. In the following iterations of the method, the steady-state solution of the non-linear system is calculated through a recursive set of linear equations, as will be shown later in the paper. At the first step it is assumed that an estimate w_{j+1} may be obtained from the previous solution w_j as

$$w_{j+1} = w_j + \left(\sum_{k=1}^{m} \frac{\partial w_j}{\partial \bar{\theta}_k} \right) \delta\bar{\theta} + \mathcal{O}\left(\delta\bar{\theta}^2\right) \approx w_j + \acute{w}_j \delta\bar{\theta} \quad (16)$$

The higher order terms $\mathcal{O}\left(\delta\bar{\theta}^2\right)$ are similarly neglected from the analysis due to their smallness. The governing equation for w_{j+1} is

$$\rho \frac{\partial^2 w_{j+1}}{\partial t^2} + c \frac{\partial w_{j+1}}{\partial t} + k\Gamma\left(w_{j+1}\right) + f_{NL}\left(w_{j+1}, \bar{\boldsymbol{\theta}}_{j+1}\right) = \frac{f}{2} \exp\left(i\Omega t\right) + cc. \quad (17)$$

Subtracting the above equation from the governing equation of motion for w_j and using Eq.(16) yields

$$\left(\rho \frac{\partial^2 \acute{w}_j}{\partial t^2} + c \frac{\partial \acute{w}_j}{\partial t} + k\Gamma\left(\acute{w}_j\right) \right) \delta\bar{\theta} + f_{NL}\left(w_{j+1}, \bar{\boldsymbol{\theta}}_{j+1}\right) - f_{NL}\left(w_j, \bar{\boldsymbol{\theta}}_j\right) = 0. \quad (18)$$

$f_{NL}\left(w_{j+1}, \bar{\boldsymbol{\theta}}_{j+1}\right)$ and $f_{NL}\left(w_j, \bar{\boldsymbol{\theta}}_j\right)$ can be calculated using Taylor's series expansion and $\bar{\boldsymbol{\theta}}_{j+1} = \left(1 + \delta\bar{\theta}\right) \bar{\boldsymbol{\theta}}_j$. After some algebraic work, Eq.(18) becomes

$$\left(\rho \frac{\partial^2 \acute{w}_j}{\partial t^2} + c \frac{\partial \acute{w}_j}{\partial t} + k\Gamma\left(\acute{w}_j\right) \right) \delta\bar{\theta} + \sum_{h=1}^{H} \left(\alpha_{(j+1)h} - \alpha_{jh} \right) w_j^h + h\alpha_{(j+1)h} w_j^{h-1} \acute{w}_j \delta\bar{\theta} = 0. \quad (19)$$

Eq.(19) is a linear function in $\acute{w}_j$. Similar to the previous step, the following solution is assumed for $\acute{w}_j$

$$\acute{w}_j = \sum_{l=1}^{L} \sum_{n=1}^{N} \varphi_n \acute{q}_{nlj} \exp\left(il\Omega t\right) + cc. \tag{20}$$

and the vector of sensitivities of steady-state amplitudes $\acute{\mathbf{q}}_j = [\acute{q}_{nlj}] \in \mathbb{R}^{NL}$ can be obtained in a similar way by solving the following linear matrix equation

$$\mathbf{A}_j \acute{\mathbf{q}}_j = \mathbf{b}_j \tag{21}$$

where $\mathbf{A}_j \in \mathbb{R}^{NL \times NL}$ and the vector $\mathbf{b}_j \in \mathbb{R}^{NL}$ will be updated at each iteration. For a system with odd non-linearity and assuming the primary harmonic responses only, we have

$$\mathbf{A}_j = \left[-\Omega^2 \mathbf{M} + i\Omega \mathbf{C} + \mathbf{K} + \mathbf{E}^{(j)}\right] \delta\bar{\theta} \tag{22}$$

where $\mathbf{E}^{(j)} = [E_{ik}^{(j)}] \in \mathbb{R}^{N \times N}$,

$$E_{ik}^{(j)} = \int_{\mathcal{D}} \sum_{h=1}^{H} \left(h\alpha_{(j+1)h} \binom{h-1}{\frac{h-1}{2}} \left(\sum_{n=1}^{N} \varphi_n q_{nj} \right)^{\frac{h-1}{2}} \left(\sum_{n=1}^{N} \varphi_n q_{nj}^* \right)^{\frac{h-1}{2}} \varphi_i \varphi_k \right) d\mathbf{r} \tag{23}$$

and the components of vector $\mathbf{b}_j = [b_{ji}] \in \mathbb{R}^N$ are

$$b_{ji} = \int_{\mathcal{D}} \sum_{h=1}^{H} \left(\left(\alpha_{jh} - \alpha_{(j+1)h}\right) \binom{h}{\frac{h-1}{2}} \left(\sum_{n=1}^{N} \varphi_n q_{nj} \right)^{\frac{h+1}{2}} \left(\sum_{n=1}^{N} \varphi_n q_{nj}^* \right)^{\frac{h-1}{2}} \right) \varphi_i d\mathbf{r} \tag{24}$$

The calculated values of $\acute{q}_{nj}$ are then inserted into Eq.(20) and the iteration continues until $\bar{\boldsymbol{\theta}} = \mathbf{1}$. It should be noted that the vector $\bar{\boldsymbol{\theta}}$ is normalised in a way that each component of vector $\boldsymbol{\theta}$ is divided by its assigned value and therefore $\bar{\boldsymbol{\theta}} = \mathbf{1}$ provides the assigned values of the non-linear control parameters. The proposed approach starts with the linear system and gradually adds non-linearity. In the case that there are multiple solutions, it is expected that the

method will most often end up at the low amplitude solution. However, there may be options for different parameters paths that can reach other solutions and including frequency as a parameter would be another option to overcome this issue (e.g. [25]). Also it should be noted that the method applies sequential perturbations in which the error will build up in the solutions. The accumulated error can be substantial in some cases, resulting in an unstable numerical process. These issues will be investigated in future work.

The above procedure may be implemented in the following steps:

1. Identify nonlinear control parameters and nondimensionalize these parameters so that they all vary from zero to one,
2. Approximate the nonlinear restoring force function using its Taylor's series (Eq.(2)),
3. Obtain the solution of the linear system at zero values of the nonlinear control parameters (Eq.(4)),
4. Balance the harmonics of interest and apply the standard Galerkin technique,
5. Set $j = 1$, obtain the steady state sensitivities of the responses at the first iteration from Eq.(12) and consequently calculate the steady state responses at the first iteration,
6. for $j = 1 : n_{\text{inc}} - 1$ (n_{inc} is the number of increments and depends on the choice of $\delta\bar{\theta}$,
   - Obtain the updated sensitivities from Eq.(21),
   - Use Eq.(16) to obtain w_{j+1} (the steady state solution at the $j+1$th iteration) from its steady state solution at the jth iteration and the updated sensitivities,
7. end.

3. Application to a Micro-Electro-Mechanical-System (MEMS)

In this section, a mathematical model of a MEMS device is used to illustrate the working of the proposed method. The model under consideration is an

isotropic micro-beam of length L, width a, thickness h, density ρ and Young's modulus E. As shown in Figure 1, four electrostatic electrodes (1, 2, 3 and 4) are located at the middle and free end of the beam. The coordinate system is attached to the middle of the left end of the beam where x and z refer to the horizontal and vertical coordinates respectively. The device is base excited at a frequency Ω and amplitude z_0.

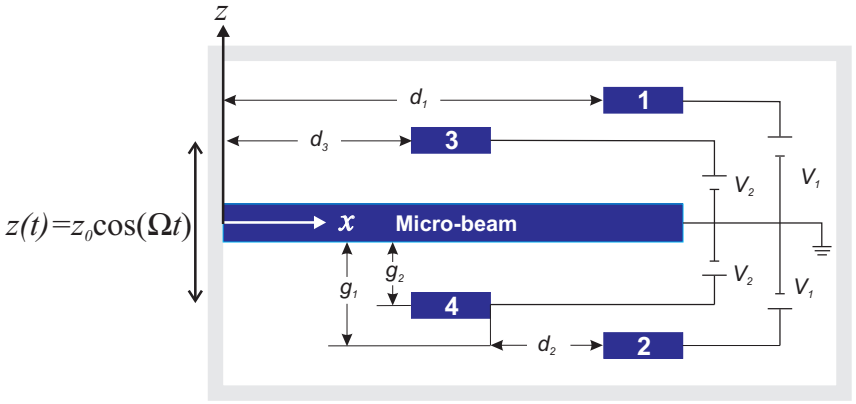

Figure 1: Schematic of the MEMS device

The beam may be modeled as an Euler-Bernoulli beam with the following governing equation

$$EI\frac{\partial^4 w(x,t)}{\partial x^4}+c_a\frac{\partial w(x,t)}{\partial t}+\rho A\frac{\partial^2 w(x,t)}{\partial t^2}=\frac{\epsilon_0 aH(x-d_1)}{2}\left(\frac{V_1^2}{(g_1-w(x,t))^2}\right)$$
$$-\frac{\epsilon_0 aH(x-d_1)}{2}\left(\frac{V_1^2}{(g_1+w(x,t))^2}\right)+\frac{\epsilon_0 a(H(x-d_2)-H(x-d_3))}{2}\left(\frac{V_2^2}{(g_2-w(x,t))^2}\right)$$
$$-\frac{\epsilon_0 a(H(x-d_2)-H(x-d_3))}{2}\left(\frac{V_2^2}{(g_2+w(x,t))^2}\right)-\rho A\frac{\partial^2 z(t)}{\partial t^2} \quad (25)$$

subject to:

$$w(0,t)=\frac{\partial w(0,t)}{\partial x}=0 \quad (26)$$
$$\frac{\partial^2 w(L,t)}{\partial x^2}=\frac{\partial^3 w(L,t)}{\partial x^3}=0 \quad (27)$$

where $w(x,t)$ is the transverse deflection of the beam relative to its base at the position x and time t, c_a is the damping coefficient, ϵ_0 is the permittivity of free space, $H(x)$ is the Heaveside function, V_1, V_2, g_1 and g_2 are the applied DC voltages and the air gaps between the electrodes located at the middle and tip (the system is assumed to be symmetric) respectively and $z(t) = z_0 \cos(\Omega t)$ is the base excitation function. In this case, the electrostatic forces cause attraction of the surfaces, hence non-linearity. Normalizing all the terms appearing in Eq.(25) and expanding the electrostatic forces in Taylor series leads to

$$\frac{\partial^4 \hat{w}(\hat{x},\hat{t})}{\partial \hat{x}^4} + c\frac{\partial \hat{w}(\hat{x},\hat{t})}{\partial \hat{t}} + \frac{\partial^2 \hat{w}(\hat{x},\hat{t})}{\partial \hat{t}^2} + \alpha_1 \hat{w} + \alpha_3 \hat{w}^3 + \mathcal{O}(\hat{w}^5) = \gamma \exp\left(i\hat{\Omega}\hat{t}\right) + cc. \quad (28)$$

where

$$\hat{w} = w/g1, \qquad \hat{x} = x/L, \qquad \hat{t} = t/T, \qquad \hat{\Omega} = \Omega T, \qquad \lambda = \frac{g_2}{g_1}$$

$$c = \frac{c_a L^4}{EIT}, \qquad T = \sqrt{\frac{\rho A L^4}{EI}}, \qquad \eta = \frac{\epsilon_0 a L^4}{EI g_1^3}, \qquad \gamma = \frac{z_0 \rho A L^4 \Omega^2}{2EI g_1}$$

$$\alpha_1 = -2\left(\eta V_{01}^2 \theta_1^2 H(\hat{x} - d_1/L) + \frac{\eta V_{02}^2 \theta_2^2 (H(\hat{x} - d_2/L) - H(\hat{x} - d_3/L))}{\lambda^3}\right)$$

$$\alpha_3 = -4\left(\eta V_{01}^2 \theta_1^2 H(\hat{x} - d_1/L) + \frac{\eta V_{02}^2 \theta_2^2 (H(\hat{x} - d_2/L) - H(\hat{x} - d_3/L))}{\lambda^5}\right)$$

and $\theta_i = V_i/V_{0i}$ $i = 1, 2$ in which V_{0i} is the maximum assigned voltage to the ith electrode. In the following analysis, we assume the micro-beam shown in Figure 1 has the characteristics introduced in Table 1. Figure 2 shows a comparison between the time responses of the non-dimensionalized tip displacement of the beam under true electrostatic forces and the truncated cubic terms of electrostatic forces. This comparison has been carried out for the conditions that the beam is excited at its first non-dimensionalized resonance frequency, i.e. $\hat{\Omega} = 2.891$ where $V_1 = V_2 = 7$ V and $z_0 = 0.1$ μm. As it can be seen in the figure, the error is about 2% which shows that the cubic non-linearity in Eq.(28)

Table 1: Geometrical and material properties of the micro-beam

Model parameter	Value
Length of the beam (L)	3000 μm
Width of the beam (a)	1000 μm
Thickness of the beam (h)	4 μm
Beam material Young's modulus (E)	169.6 GPa
Beam material density (ρ)	2330 kg/m
Viscous damping coefficient (c)	0.003 N.s/m^3
Permittivity component (ϵ_0)	13.48 nF/m
g_1	30 μm
g_2	15 μm

is the most significant non-linear term for the given amplitude of excitation and the voltages. By increasing the voltages the error will be greater as the system will become close to its unstable point. At a certain voltage, known as the pull-in voltage in the literature of MEMS devices, the system loses its stability. In this paper, the applied DC voltages are lower than the pull-in voltage and therefore the pull-out voltage (the voltage at which the micro-switch electrodes lose contact after pull-in occurs [31]) is not considered. The errors in the parameters of the MEMS model shown in Figure 1 are neglected. This is because the main concern of this paper is on the application of the method to an example nonlinear dynamics problem. However, in many real applications of MEMS [32, 33, 34], parametric errors affect the pull in voltage and therefore should be taken into account. Three different cases are considered for calculating pull-in voltage as will be described in the followings. It should be noted that, hereafter, the effects of the 5th and higher order terms of electrostatic forces are ignored.

The method described in Section 2 is now illustrated in the above example of a micro-beam with nonlinear electrostatic force. Comparing Eq.(28) to Eq.(1) and Eq.(2), we have $k = 1$, $\rho = 1$, $\Gamma \equiv \frac{\partial^4}{\partial x^4}$, $f = 2\gamma$ and $\mathcal{D} = \{\hat{x} \in \mathbb{R} : 0 \leq \hat{x} \leq 1\}$. The first two modes of the beam are considered for the

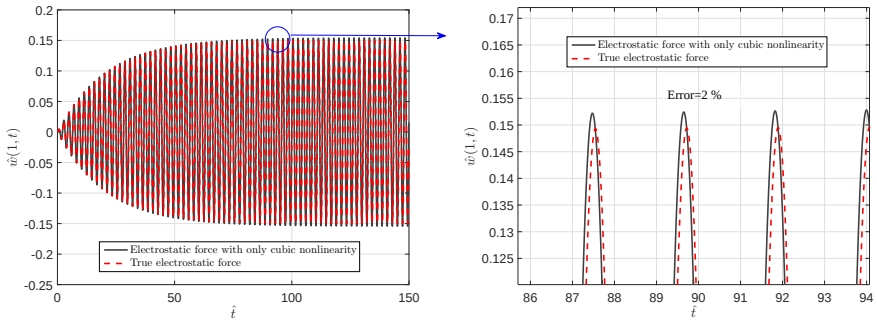

(a) Time histories (b) Zoomed area

Figure 2: Non-dimensionalized tip displacement time histories for the system with only cubic non-linearity (solid line) and the system with true electrostatic force (dashed line), $V_1 = V_2 = 7$ V, $z_0 = 0.1$ μm, $\hat{\Omega} = 2.891$.

analysis, hence $N = 2$. The mode shapes of a clamped-free beam having unit length are

$$\varphi_n(\hat{x}) = \cosh(\beta_n \hat{x}) - \cos(\beta_n \hat{x}) + \left(\frac{\cos(\beta_n) + \cosh(\beta_n)}{\sin(\beta_n) - \sinh(\beta_n)}\right)(\sin(\beta_n \hat{x}) - \sinh(\beta_n \hat{x})) \tag{29}$$

where $\beta_1 = 1.87510407$ and $\beta_2 = 4.69409113$. Knowing that the system has only cubic non-linearity ($H = 3$) and assuming the primary harmonic responses only ($L = 1$), $\mathbf{A}_1 \in \mathbb{R}^{2\times 2}$, $\mathbf{b}_1 \in \mathbb{R}^2$, $\mathbf{A}_j \in \mathbb{R}^{2\times 2}$ and $\mathbf{b}_j \in \mathbb{R}^2$ can be calculated according to Eq.(13), Eq.(15), Eq.(22) and Eq.(24) respectively. In this example, the nonlinear control parameters are assumed as $\theta_1 = V_1/V_{01}$ and $\theta_2 = V_2/V_{02}$ where V_{01} and V_{02} are the maximum voltages that can be applied to the system. Three different case studies are considered in this section. The first case is when all electrodes are included in the circuit, while in the second case electrodes 3 and 4 are disconnected from the circuit, hence $\theta_2 = 0$ and finally electrodes 1 and 2 will be removed in the third case in which $\theta_1 = 0$. In case 1 the solutions obtained by the proposed method are validated using numerical integration results.

3.1. Case 1

The validation of the proposed method is first investigated. Figure 3 shows the tip displacement frequency response for modes 1 and 2 at different voltages, and demonstrates that the results obtained by the proposed method agree well with those obtained by numerical integration. The results also showed that the proposed method is capable of predicting the frequency response of a nonlinear system with a strong but smooth non-linearity (high voltages).

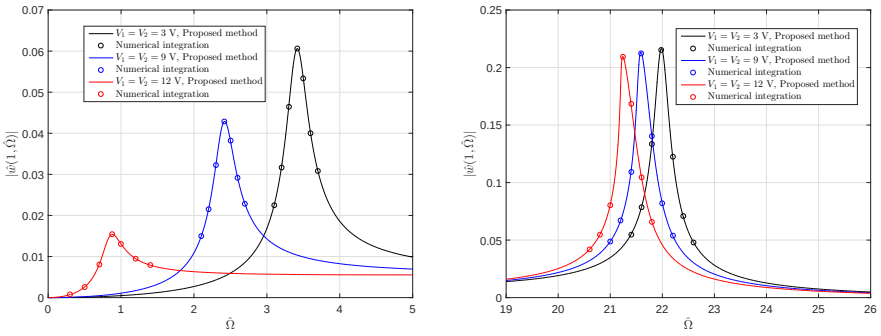

(a) (b)

Figure 3: Validation of the results (a) mode 1 and (b) mode 2.

To calculate the pull-in voltage in this case, both V_1 and V_2 are gradually and equally increased at different frequencies and the solution is sought using numerical integration. This is shown in Figure 4 where the beam tip displacement time histories at $V_1 = V_2 = 12.3$ V and $V_1 = V_2 = 12.4$ V are shown. As can be seen in the figure, the displacement grows unboundedly once $V_1 = V_2 = 12.4$ V. Therefore the analysis is carried out for voltages between 0 and 12 V in this case.

Figure 5 shows the frequency response of the tip-displacement of the beam in case 1, obtained by the proposed method. The results show that increasing the voltages V_1 and V_2 from zero to 12 V, that is changing the non-dimensionalised voltages θ_1 and θ_2 from 0 to 1, affects the dynamic characteristics of the beam. One can use this effect to control the vibration responses of the MEMS device. By applying the DC voltages, the natural frequencies of the beam are changed.

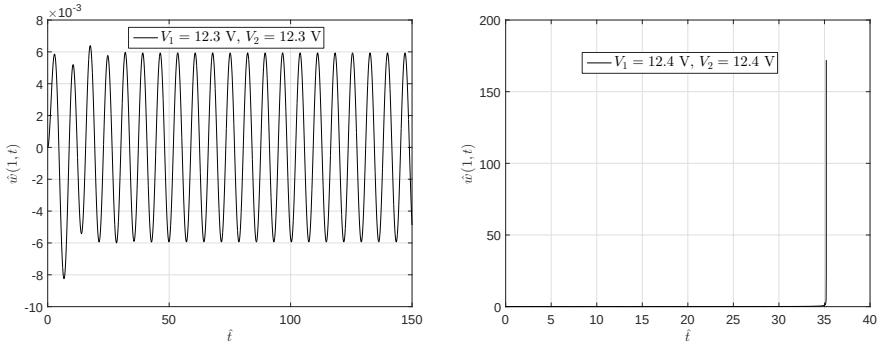

(a) (b)

Figure 4: Non-dimensionalized tip displacement time histories at $\hat{\Omega} = 0.873$ and (a) $V_1 = V_2 = 12.3$ V and (b) $V_1 = V_2 = 12.4$ V.

The proposed method is capable of calculating the sensitivities of the responses with respect to voltages and therefore an inverse problem can be readily formulated to assign the desired natural frequencies of the MEMS. Table 2 shows the nondimensional natural frequencies of the system at different voltages. As indicated in the table, the variation in the first resonance frequency is much more significant than mode 2. The results show that the first resonance frequency is decreased by 75% while the second resonance frequency only reduces by 3.6%. This is expected as the second mode has higher dynamic stiffness and higher voltages are required to change its resonance frequency, but this is limited to the pull-in voltages that affect the first mode simultaneously. It will be shown that by removing electrodes 1 and 2, case 3, a slightly higher decrease in the second resonance frequency can be achieved. Obtaining optimal locations of the electrodes and suitable gaps between the electrodes and the micro-beam can help to improve the controllability of the second mode. However, this is beyond the scope of this paper and can be investigated in future work.

The summation of sensitivities of the beam-tip displacement in the frequency domain and its phase plot are shown in Figure 6. Two sets of interesting results have emerged from this figure. First, it can be seen that the sensitivities are increasing as the voltages rise and reach maximum at $V_1 = V_2 = 12$ V, i.e. near

Table 2: Changes in nondimensional natural frequencies (case 1)

Voltages	Resonance frequency Mode 1	Resonance frequency Mode 2
$V_1 = V_2 = 0$ V	3.52	22.03
$V_1 = V_2 = 3$ V	3.41	21.98
$V_1 = V_2 = 6$ V	3.08	21.88
$V_1 = V_2 = 9$ V	2.42	21.59
$V_1 = V_2 = 12$ V	0.88	21.24

the instability. This has been reported in the literature for other applications (e.g. flutter instability [35]). The second interesting feature in Figure 6 is the presence of anti-resonance points in the vicinity of the non-dimensionalised frequency of $\hat{\Omega} = 15$. This provides the designer with valuable information with which to improve the robustness with respect to uncertainties of the system. Based on the information in Figure 5, the optimal excitation frequency range, i.e. the region of frequency in which the vibration amplitude is minimal, is within $\hat{\Omega} \in [5, 20]$. However, the robust optimal frequency range can be considered in the range of $\hat{\Omega} = 14$ to $\hat{\Omega} = 16$ where the sensitivities are minimal and therefore any change in the voltages does not result in significant increase in the vibration amplitude. As mentioned earlier, the sensitivities can also be used in an inverse problem in order to change the dynamic characteristics of the system in a desirable way.

3.2. Case 2

In this case, electrodes 3 and 4 are disconnected from the system. Therefore, only the voltage source V_1 is active. In order to determine how much this voltage can be increased, the solution of the system is numerically found at different voltages and, as shown in Figure 7, the beam becomes unstable at $V_1 = 18.8$ V. Therefore, V_1 varies from 0 to 18 V in this case.

The frequency and phase responses of the beam-tip displacement are plotted in Figure 8. Similar to the previous case, the first and second natural frequencies

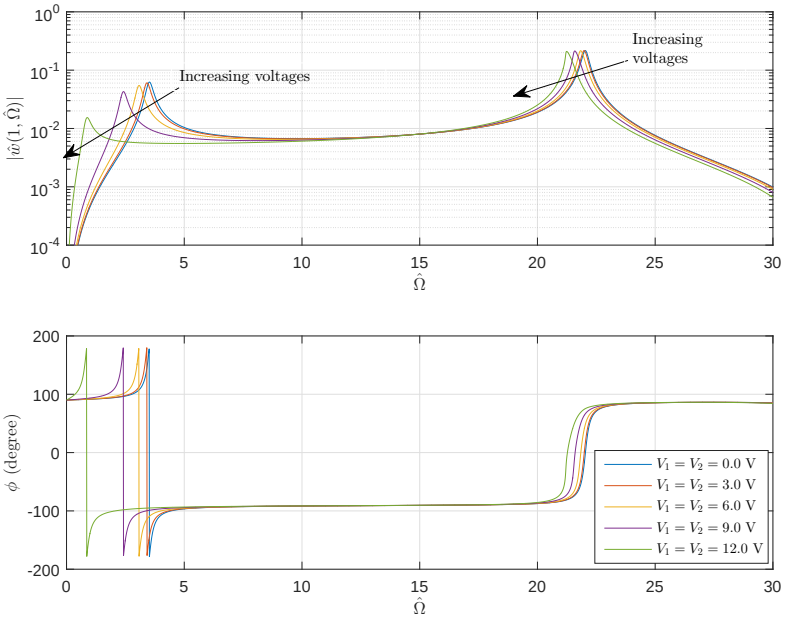

Figure 5: Frequency and phase responses of the beam-tip displacement (case 1).

of the system falls when the voltage increases. However, as indicated in Table 3, the change in the second resonance frequency is almost negligible as it decreases by only 1.32%. The variation of the first natural frequency, when V_1 increases from 0 V to 18 V, is more noticeable, that is 71.88%. This indicates that the dynamic characteristic of the first mode can be modified by only the presence of the tip electrodes. This is due to the fact that adding the middle electrodes provides slightly more capability to decrease the resonance frequency, i.e. from 71.88% (case 2) to 75% (case 1).

As shown in Figure 9, a similar behaviour for the sensitivity of the frequency response of the tip displacement with respect to V_1 is observed as the previous case. However, the range of robust optimal excitation frequency has been moved further up the frequency axis. From the figure, one may conclude that the robust optimal excitation frequency range is between $\hat{\Omega} = 17$ and $\hat{\Omega} = 19$.

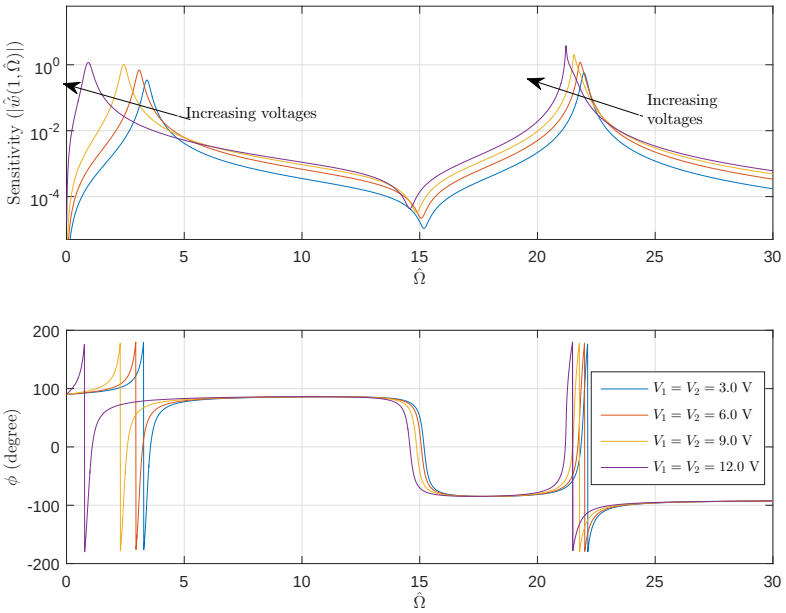

Figure 6: Sum of sensitivities of frequency and phase responses of the beam-tip displacement with respect to V_1 and V_2 (case 1).

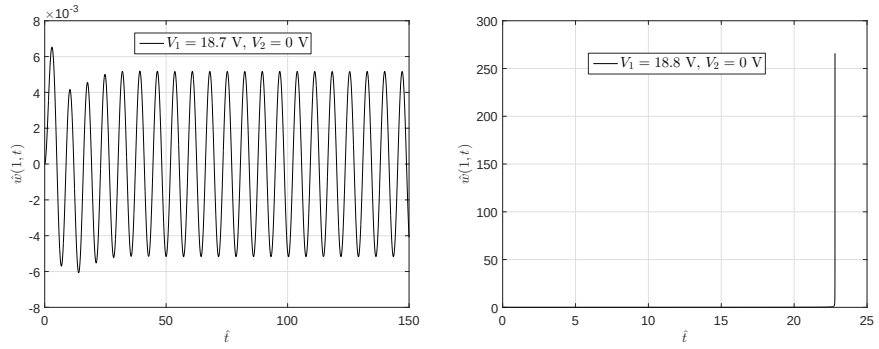

(a) (b)

Figure 7: Non-dimensionalized tip displacement time histories at $\hat{\Omega} = 0.873$ and (a) $V_1 = 18.7$ V, $V_2 = 0$ V and (b) $V_1 = 18.8$ V, $V_2 = 0$ V.

3.3. Case 3

Finally, electrodes 1 and 2 are removed from the beam and V_2 becomes the only active voltage source. As shown in Figure 10, the pull-in voltage is 16.5 V

Table 3: Changes in nondimensional natural frequencies (case 2)

Voltages	Resonance frequency Mode 1	Resonance frequency Mode 2
$V_1 = 0.0$ V	3.52	22.03
$V_1 = 4.5$ V	3.42	22.01
$V_1 = 9.0$ V	3.09	21.96
$V_1 = 13.5$ V	2.44	21.87
$V_1 = 18.0$ V	0.99	21.74

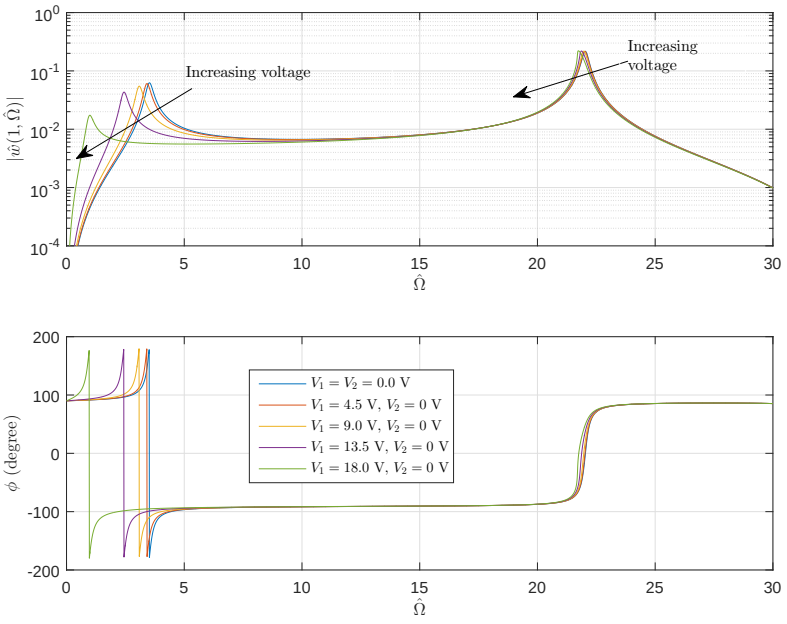

Figure 8: Frequency and phase responses of the beam-tip displacement (case 2).

and this is expected as the gap g_2 is half of g_1 (Table 1). In this case, V_2 varies from 0 to 16 V and the beam tip displacement and its sensitivity with respect to V_2 are plotted in the frequency domain and these results are shown in Figures 11 and 12. As can be see in Figure 10 and Table 4, the change in natural frequencies

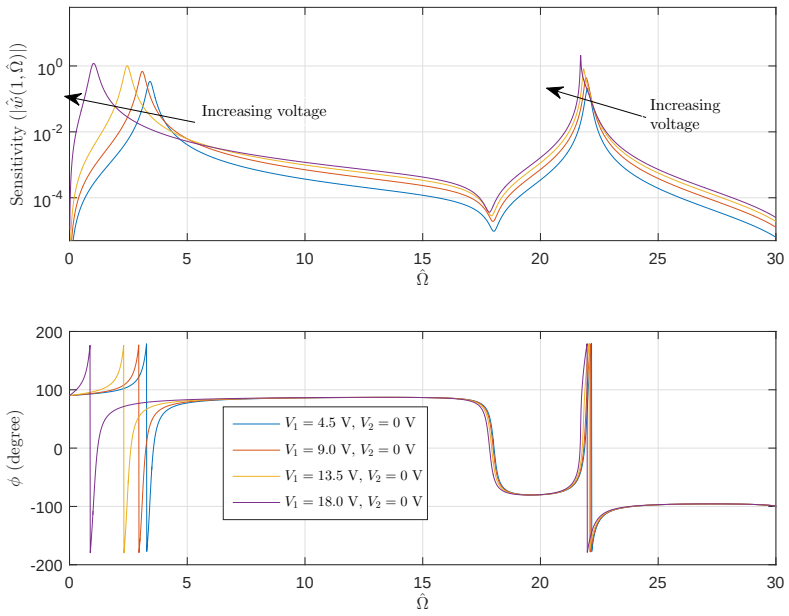

Figure 9: Sensitivity of frequency and phase responses of the beam-tip displacement with respect to V_1 (case 2).

are greater than the previous two cases, being decreases of 75.28% and 5.14% respectively. This indicates that case 3 can be considered as the most effective case in changing the dynamic characteristics of the system, when compared to cases 1 and 2. Only three test cases are considered in this paper to demonstrate the working of the proposed method. However, the optimal case can be obtained through an optimization problem, depending on the objectives that are desired. Figure 12 indicates the sensitivity of the beam tip displacement with respect to V_2. The figure shows similar behaviour as those of the previous cases, i.e. cases 1 and 2. The only difference is the fact that the anti-resonance frequency is moved towards the left and the region of antiresonance frequencies is now from 12 Hz to 14 Hz. As already mentioned in the paper, the information in the frequency response of the sensitivities will be useful in obtaining the robust

Table 4: Changes in nondimensional natural frequencies (case 3)

Voltages	Resonance frequency Mode 1	Resonance frequency Mode 2
$V_1 = 0.0$ V	3.52	22.03
$V_1 = 4.5$ V	3.42	21.96
$V_1 = 9.0$ V	3.08	21.74
$V_1 = 13.5$ V	2.42	21.37
$V_1 = 18.0$ V	0.87	20.84

optimal excitation frequencies. However, depending on the application, these regions have to be avoided if the objective is to control the dynamic response of the system using the applied DC voltages.

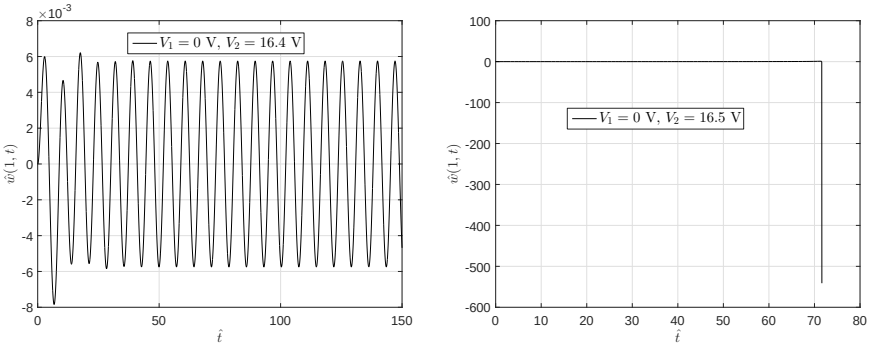

(a) (b)

Figure 10: Non-dimensionalized tip displacement time histories at $\hat{\Omega} = 0.873$ and (a) $V_1 = 0$ V, $V_2 = 16.4$ V and (b) $V_1 = 0$ V, $V_2 = 16.5$ V.

4. Conclusion

An extended Harmonic Balance method for the calculation of steady state responses of nonlinear dynamic systems and their sensitivities with respect to nonlinear control parameters is formulated. The method assumes that the approximate nonlinear restoring force functions can be obtained through a limited number of polynomial terms, calculated from the Taylor series expansions.

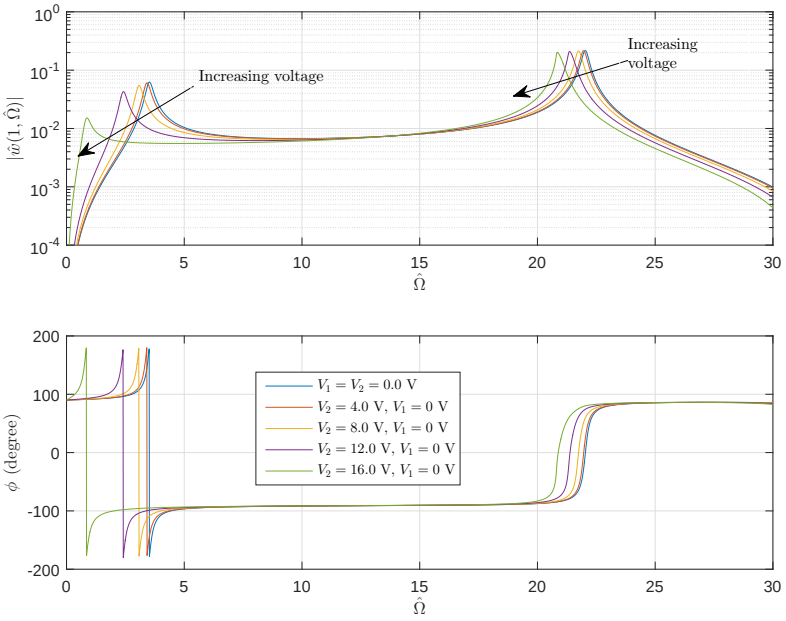

Figure 11: Frequency and phase responses of the beam-tip displacement (case 3).

Based on this assumption, the nonlinear restoring function can be controlled by a set of so called 'nonlinear control parameters'. The system is linear when these nonlinear control parameters are zero. This property is used to obtain steady state solution of the nonlinear dynamic problem together with the sensitivities of the solution with respect to these parameters by incrementing them from zero to their assigned values. It is shown that two sets of linear equations are required. The first set of equations is obtained by perturbing the system from its linear state. This equation provides the frequency response of the summation of sensitivities of the weakly-nonlinear system with respect to the nonlinear control parameters. From the second iteration, a general form of recursive linear equations are derived which give the summation of sensitivities with respect to the nonlinear control parameters. The proposed method has the following advantages:

- It simultaneously obtains the steady state responses of multi-dimensional

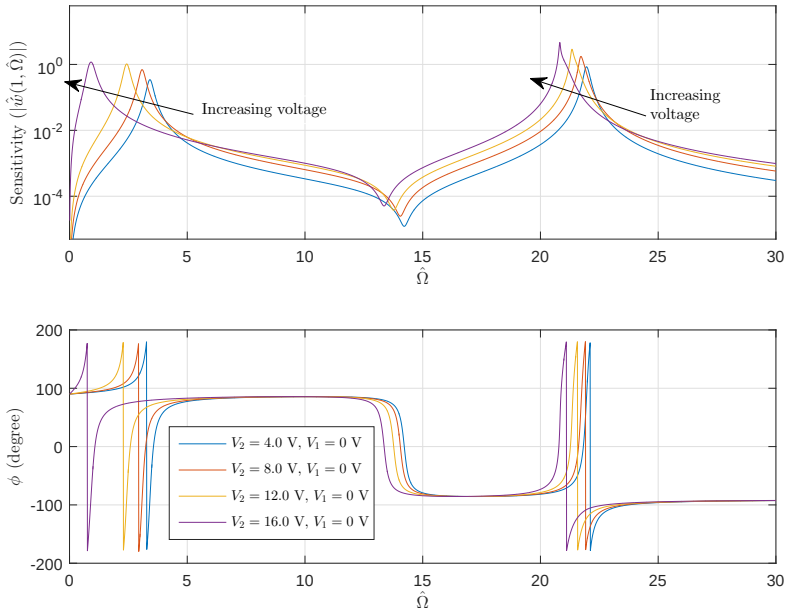

Figure 12: Sensitivity of frequency and phase responses of the beam-tip displacement with respect to V_2 (case 3).

nonlinear dynamic systems and their sensitivities with respect to nonlinear control parameters by only solving linear equations.

- The method can be applied to multi-degree of freedom systems with any order of smooth nonlinearity.

- The method is capable of determining the steady-state solution of higher order harmonies together with their sensitivities with respect to nonlinear control parameters.

The proposed method is demonstrated in numerical simulations of a MEMS device with nonlinear electrostatic forces. The nonlinear control parameters are assumed to be the applied DC voltages that control the dynamics of the system. Some interesting features, such as a significant increase in the sensitivities of the MEMS responses in the vicinity of unstable points and the anti-resonance

frequencies of the sensitivities, are observed and discussed. The method is validated using numerical integration.

Future work will involve including frequency as a parameter, investigating the effects of different parameter paths on the solution, the extension of the proposed method to nonlinear aeroelastic systems, and the application of the method to vibration control and robust design.

Acknowledgment

Financial support from the Royal Academy of Engineering (ISS1516-8-21) and the Sêr Cymru National Research Network (NRNC28) through industrial secondment award is gratefully acknowledged. Hadi Madinei acknowledges the financial support from the Swansea University through the award of the Zienkiewicz scholarship.

References

[1] Q. Mao, S. Pietrzko, Design of shaped piezoelectric modal sensor for beam with arbitrary boundary conditions by using adomian decomposition method, Journal of Sound and Vibration 329 (11) (2010) 2068 – 2082.

[2] J.-J. Li, C.-J. Cheng, Differential quadrature method for analyzing nonlinear dynamic characteristics of viscoelastic plates with shear effects, Nonlinear Dynamics 61 (1–2) (2010) 57–70.

[3] S. Azizi, M. Ghazavi, G. Rezazadeh, I. Ahmadian, C. Cetinkaya, Tuning the primary resonances of a micro resonator, using piezoelectric actuation, Nonlinear Dynamics 76 (1) (2014) 839–852.

[4] S. Faroughi, H. H. Khodaparast, M. I. Friswell, Non-linear dynamic analysis of tensegrity structures using a co-rotational method, International Journal of Non-Linear Mechanics 69 (2015) 55 – 65.

[5] D. J. Wagg, S. A. Neild, Nonlinear vibration with control: for flexible and adaptive structures, Vol. 218, Springer, 2014.

[6] D.-Q. Zeng, Nonlinear oscillator with discontinuity by the maxmin approach, Chaos, Solitons & Fractals 42 (5) (2009) 2885 – 2889.

[7] S.-Q. Wang, J.-H. He, Nonlinear oscillator with discontinuity by parameter-expansion method, Chaos, Solitons & Fractals 35 (4) (2008) 688 – 691.

[8] D. Younesian, H. Askari, Z. Saadatnia, M. KalamiYazdi, Frequency analysis of strongly nonlinear generalized duffing oscillators using hes frequencyamplitude formulation and hes energy balance method, Computers & Mathematics with Applications 59 (9) (2010) 3222 – 3228.

[9] J.-H. He, Variational iteration methodsome recent results and new interpretations, Journal of Computational and Applied Mathematics 207 (1) (2007) 3 – 17.

[10] X. Gu, W. Zhu, A stochastic averaging method for analyzing vibro-impact systems under gaussian white noise excitations, Journal of Sound and Vibration 333 (9) (2014) 2632 – 2642.

[11] M. Sheikhlou, R. Shabani, G. Rezazadeh, Nonlinear analysis of electrostatically actuated diaphragm-type micropumps, Nonlinear Dynamics 83 (1-2) (2016) 951–961.

[12] T. Burton, A perturbation method for certain non-linear oscillators, International Journal of Non-Linear Mechanics 19 (5) (1984) 397–407.

[13] L. Xu, He's parameter-expanding methods for strongly nonlinear oscillators, Journal of Computational and Applied Mathematics 207 (1) (2007) 148 – 154.

[14] Y. Qian, D. Ren, S. Lai, S. Chen, Analytical approximations to nonlinear vibration of an electrostatically actuated microbeam, Communications in Nonlinear Science and Numerical Simulation 17 (4) (2012) 1947 – 1955.

[15] S. Shahlaei-far, A. Nabarrete, J. M. Balthazar, Nonlinear vibrations of cantilever timoshenko beams: a homotopy analysis, Latin American Journal of Solids and Structures, an ABCM Journal 13 (10) (2016) 1866–1877.

[16] I. Mehdipour, D. Ganji, M. Mozaffari, Application of the energy balance method to nonlinear vibrating equations, Current Applied Physics 10 (1) (2010) 104 – 112.

[17] S. C. Stanton, B. A. Owens, B. P. Mann, Harmonic balance analysis of the bistable piezoelectric inertial generator, Journal of Sound and Vibration 331 (15) (2012) 3617 – 3627.

[18] T. K. Caughey, Equivalent linearization techniques, The Journal of the Acoustical Society of America 35 (11) (1963) 1706–1711.

[19] K. Fujimura, A. D. Kiureghian, Tail-equivalent linearization method for nonlinear random vibration, Probabilistic Engineering Mechanics 22 (1) (2007) 63–76.

[20] R. Puenjak, Extended lindstedtpoincare method for non-stationary resonances of dynamical systems with cubic nonlinearities, Journal of Sound and Vibration 314 (12) (2008) 194 – 216.

[21] S. Chen, Y. Cheung, A modified lindstedt-poincaré method for a strongly nonlinear system with quadratic and cubic nonlinearities, Shock and vibration 3 (4) (1996) 279–285.

[22] I. Kovacic, Forced vibrations of oscillators with a purely nonlinear power-form restoring force, Journal of Sound and Vibration 330 (17) (2011) 4313 – 4327.

[23] M. Fesanghary, T. Pirbodaghi, M. Asghari, H. Sojoudi, A new analytical approximation to the duffing-harmonic oscillator, Chaos, Solitons & Fractals 42 (1) (2009) 571 – 576.

[24] Z. Peng, G. Meng, Z. Lang, W. Zhang, F. Chu, Study of the effects of cubic nonlinear damping on vibration isolations using harmonic balance method, International Journal of Non-Linear Mechanics 47 (10) (2012) 1073 – 1080.

[25] Y. Cheung, S. Chen, S. Lau, Application of the incremental harmonic balance method to cubic non-linearity systems, Journal of Sound and Vibration 140 (2) (1990) 273 – 286.

[26] K. Sze, S. Chen, J. Huang, The incremental harmonic balance method for nonlinear vibration of axially moving beams, Journal of Sound and Vibration 281 (35) (2005) 611 – 626.

[27] S. Lai, C. Lim, B. Wu, C. Wang, Q. Zeng, X. He, Newtonharmonic balancing approach for accurate solutions to nonlinear cubicquintic duffing oscillators, Applied Mathematical Modelling 33 (2) (2009) 852 – 866.

[28] A. Grolet, F. Thouverez, On a new harmonic selection technique for harmonic balance method, Mechanical Systems and Signal Processing 30 (2012) 43 – 60.

[29] Z. Guo, X. Ma, Residue harmonic balance solution procedure to nonlinear delay differential systems, Applied Mathematics and Computation 237 (2014) 20 – 30.

[30] P. Ju, X. Xue, Global residue harmonic balance method to periodic solutions of a class of strongly nonlinear oscillators, Applied Mathematical Modelling 38 (24) (2014) 6144 – 6152.

[31] H. Samaali, F. Najar, S. Choura, A. H. Nayfeh, M. Masmoudi, A double microbeam mems ohmic switch for rf-applications with low actuation voltage, Nonlinear Dynamics 63 (4) (2011) 719–734.

[32] J. M. Balthazar, D. G. Bassinello, A. M. Tusset, Á. M. Bueno, B. R. de Pontes Junior, Nonlinear control in an electromechanical transducer with chaotic behaviour, Meccanica 49 (8) (2014) 1859–1867.

[33] N. Peruzzi, F. Chavarette, J. Balthazar, A. Tusset, A. Perticarrari, R. Brasil, The dynamic behavior of a parametrically excited time-periodic mems taking into account parametric errors, Journal of Vibration and Controldoi:10.1177/1077546315573913.

[34] A. M. Tusset, J. M. Balthazar, D. G. Bassinello, B. R. Pontes, J. L. P. Felix, Statements on chaos control designs, including a fractional order dynamical system, applied to a "mems" comb-drive actuator, Nonlinear Dynamics 69 (4) (2012) 1837–1857.

[35] H. H. Khodaparast, J. E. Mottershead, K. J. Badcock, Propagation of structural uncertainty to linear aeroelastic stability, Computers & Structures 88 (3–4) (2010) 223–236.